HHS Public Access

Author manuscript

Curr Biol. Author manuscript; available in PMC 2018 December 18.

Published in final edited form as:

Curr Biol. 2017 December 18; 27(24): 3826–3836.e5. doi:10.1016/j.cub.2017.11.023.

Origins and specification of the *Drosophila* wing

David Requena[1], **Jose Andres Álvarez**[2], **Hugo Gabilondo**[1], **Ryan Loker**[3], **Richard S. Mann**[3,*], and **Carlos Estella**[1,4,*]

[1]Departamento de Biología Molecular and Centro de Biología Molecular Severo Ochoa, Universidad Autónoma de Madrid (UAM), Nicolás Cabrera 1, 28049 Madrid, Spain

[2]Departamento Biología and Centro de Biología Molecular Severo Ochoa, Universidad Autónoma de Madrid (UAM), Nicolás Cabrera 1, 28049 Madrid, Spain

[3]Departments of Biochemistry and Molecular Biophysics and Systems Biology, Mortimer B. Zuckerman Mind Brain Behavior Institute, Columbia University, 701 W. 168th St., HHSC 1104, New York, NY 10032, USA

Summary

The insect wing is a key evolutionary innovation that was essential for insect diversification. Yet despite their importance, there is still debate about their evolutionary origins. Two main hypotheses have been proposed: the paranotal hypothesis suggests that wings evolved as an extension of the dorsal thorax, while the gill-exite hypothesis proposes that wings were derived from a modification of a pre-existing branch at the dorsal base (subcoxa) of the leg. Here we address this question by studying how wing fates are initially specified during *Drosophila* embryogenesis, by characterizing a *cis*-regulatory module (CRM) from the *snail* (*sna*) gene, *sna*-DP (for dorsal primordia). *sna*-DP specifically marks the early primordia for both the wing and haltere, collectively referred to as the dorsal primordia. We found that the inputs that activate *sna*-DP are distinct from those that activate *Distalless*, a marker for leg fates. Further, in genetic backgrounds in which the leg primordia are absent, the dorsal primordia are still partially specified. However, lineage-tracing experiments demonstrate that cells from the early leg primordia contribute to both ventral and dorsal appendage fates. Together, these results suggest that the wings of *Drosophila* have a dual developmental origin: two groups of cells, one ventral and one more dorsal, give rise to the mature wing. We suggest that the dual developmental origins of the wing may be a molecular remnant of the evolutionary history of this appendage, in which cells of the subcoxa of the leg coalesced with dorsal outgrowths to evolve a dorsal appendage with motor control.

[*]Corresponding authors: Richard S. Mann, rsmann10@gmail.com +1-212-305-7731. Carlos Estella, cestella@cbm.csic.es +34-91-196-4436.

[4]Lead Contact

Author Contributions:

D.R, J.A.A, H.G, R.L, and C.E performed the experiments. D.R, J.A.A, H.G, R.L, C.E and R.S.M. analyzed the data. C.E. and R.S.M. wrote the manuscript.

eTOC blurb

By studying a *cis*-regulatory module that is specifically active in the embryonic dorsal (wing and haltere) primordia of *Drosophila*, Requena et al demonstrate that dorsal fates are derived from two separate groups of cells, one that shares a lineage with the ventral primordia. These data are consistent with a dual evolutionary origin of the wing.

Keywords

Insect wing evolution; appendage development; wing primordia; haltere primordia; *Drosophila* development; leg primordia; embryogenesis; Wingless; Decapentaplegic

Introduction

It is estimated that nearly three quarters of the species currently living on Earth are insects. Although there have been several hypotheses to explain this vast diversity, one likely contributing factor was the acquisition of flight due to the development of wings approximately 350 million years ago, long before any vertebrate acquired the ability to fly [1, 2]. Yet despite their importance to life on Earth, there is still debate about the evolutionary origins of insect wings [3]. One set of ideas, collectively termed the paranotal hypothesis, suggests that wings evolved as an extension from a part of the dorsal thorax called the thoracic tergum, or paranotal lobe [4, 5]. According to this hypothesis, this anatomical outgrowth initially gave insects the ability to glide, creating the opportunity for the evolution of wing anatomy and function. However, the paranotal lobe was unlikely to have any musculature or neural innervation, raising significant questions about how motor control of these dorsal outgrowths would have evolved. An alternative hypothesis proposes that wings were derived from a modification of a pre-existing branch at the dorsal base of the leg, a region referred to as the subcoxa [6–10]. In aquatic arthropods this structure may have initially evolved as a gill, specializing in gas exchange, and was subsequently modified to become a wing following terrestrialization of some crustacean lineages.

Two principal approaches have informed our current view of insect wing evolution. One approach, which depends on careful examination of the fossil record to trace the origins of the wing, has provided support for both a paranotal lobe and subcoxa origin [5–7, 11]. One limitation of this approach is that there is a large gap in the fossil record that spans the period of time when wings first appeared. An alternative approach relies on comparing the expression patterns of molecular markers of appendages in extant insects and crustaceans that may represent early steps of wing evolution [3]. Using this approach, for example, genes that are expressed in the developing wing of *Drosophila melanogaster* were also found to be expressed in the subcoxal gills of branched appendages in two different crustaceans, consistent with a subcoxal origin for the insect wing [8, 12]. Although compelling, these types of studies also have their limitations. For one, the presence of similar markers in the fly wing and non-wing structures such as the crustacean gill could represent examples of convergent, instead of divergent, evolution. Second, many of the markers used in these studies are expressed in both leg and wing precursors, or at late stages of development, making them less definitive [13]. More recently, in two insects wing markers were found to

be expressed in two separate domains, corresponding to the positions of dorsal outgrowths and subcoxal branches, providing evidence for the idea that wings evolved from a fusion of these two initially distinct structures [3, 14, 15]. This dual origin hypothesis has also been supported by functional studies and recent fossil analysis [11, 16–18].

A complementary approach that may help inform the origins of insect appendages are experiments that characterize how the wing and leg primordia are initially specified during development using *cis*-regulatory modules (CRMs) that are active in the appendage primordia. These CRMs are not only useful as markers, but they can be used to genetically label and trace the progeny of these primordia. For example, the characterization of an early CRM from the *Distalless* (*Dll*) gene in *Drosophila* called *Dll304* has already provided evidence for a subcoxal origin of the wing [19, 20]. Although *Dll* function is not required for the establishment of wing fates, *Dll304* is active in a group of ~30 ventral cells early in embryogenesis, and the progeny of these cells contributes to both the ventral (leg) and dorsal (wing and haltere) appendages [20, 21]. Slightly later in embryogenesis, a different *Dll* CRM called *DllLT* is active in a subset of the cells that previously expressed *Dll304* [19–21]. Unlike *Dll304*, *DllLT*-expressing cells only give rise to part of the leg and do not contribute to dorsal appendages [21, 22]. In sum, these experiments reveal that *Dll*-expressing ventral cells in the early embryo contribute to both leg and wing fates, but soon thereafter the only adult structure that *Dll*-expressing cells give rise to is legs (reviewed in [23]).

To the extent that developmental studies in extant organisms can be used to inform evolution, these findings are consistent with a shared evolutionary origin of legs and wings. However, an important but currently missing test of this idea is to characterize CRMs that are specifically active in the dorsal (wing and haltere) primordia (DP). Although several genes, including *vestigial* (*vg*), *snail* (*sna*), and *escargot* (*esg*), are well known embryonic markers of the DP in *Drosophila*, no CRMs have yet been described that specifically label these cells [24–29]. Here we describe the first such CRM that is specifically active in both the wing and haltere primordia during *Drosophila* embryogenesis. We use this CRM, derived from the *sna* gene, to analyze the signals and transcription factors that are required for the specification of the DP. We find that the inputs that activate this CRM are distinct from those that activate *Dll*, suggesting that the DP are, at least in part, specified independently of the ventral (leg) primordia (VP). Moreover, in genetic backgrounds in which the VP are absent or ablated, DP fates are still partially specified. Together, these results demonstrate that the dorsal appendages of *Drosophila* have a dual developmental origin: although some DP cells share a lineage with the VP, much of the DP is independently derived from non-VP cells. Based on these developmental data in *Drosophila*, we discuss the idea of a dual evolutionary origin of wings, in which cells of the subcoxa migrated and coalesced with dorsal outgrowths to evolve a dorsal appendage with motor control.

Results

Identification of the *sna*-DP CRM

The formation of the wing and haltere primordia requires the function of *sna* and *esg* [27]. Although *sna* expression is restricted to the DP, *esg* is also expressed in the VP [24–27]

(Figure 1B and 2A). Therefore, we searched for CRMs of the *sna* gene specifically active in the DP.

Although multiple *sna* CRMs have been identified [30–32], none of them drive expression in the DP. An unbiased scan of the locus identified a single fragment that had such activity; notably, this fragment overlaps with VT7914 from the Vienna *Drosophila* Resource Center (VDRC) that also shows activity in the DP (Figure 1A). We named this CRM *sna*-DP and used it to drive *lacZ* reporter genes and compare its activity with *Dll* during embryonic development (Figure 1B). *sna*-DP was first detected at stage 12/13 in a few cells dorsal to *Dll* expressing cells in the second and third thoracic segment (T2 and T3) and, by stage 14, the number of *sna*-DP cells in T2 and T3 increased to an average number of 20 and 14 cells, respectively. The *sna*-DP reporter overlaps perfectly with Sna and Vg protein (Figure S1). Like *sna*, *sna*-DP is not active in third instar imaginal discs. However, cell-lineage tracing experiments using a minimized version of *sna*-DP (*sna*-1.7; see below) efficiently labeled the entire wing and haltere imaginal discs and a small number of proximal cells of all three leg discs in third instar larvae (Figure 1C and Figure S2). Thus, *sna*-DP marks DP cells that will give rise to the dorsal regions of the T2 and T3 segments of the adult, including the wing and haltere appendages, respectively.

Partially independent origins of the dorsal and ventral primordia

Because of the shared lineages for the ventral and dorsal appendage primordia [20, 21, 33], we investigated the relationship between these primordia using *sna*-DP as a marker. First, we compared the spatial and temporal expression pattern between cells that had expressed *Dll*, using Dll^{MD23}-*Gal4*; UAS-*GFP* (*Dll>GFP*), and the *sna*-DP reporter (Figure 1E). The perdurance of Gal4 and GFP allowed us to trace the cells that had activated, but no longer actively transcribe, *Dll*. The initial activation of *sna*-DP at stage 12/13 was observed primarily in *Dll>GFP* cells, while at stage 14 approximately half of the *sna*-DP-expressing cells were also labeled with *Dll>GFP* (Figure 1E, F and Movie S1), consistent with *Dll* lineage tracing experiments (Figure 1D and Figure S2). Although *Dll*-expressing cells can give rise to all regions of the third instar wing disc, individual wing discs are only partially labeled and there is a bias for these cells to populate the ventral portion of the disc (Figure 1D and Figure S2). The partial labeling of the wing discs by Dll^{MD23}-*Gal4* contrasts with near 100% labeling of the leg imaginal discs, arguing that it is unlikely due to a low efficiency of the lineage tracing method. Curiously, lineage tracing with the early *Dll304* CRM, which is only active early and transiently, reveals a bias for labeling the anterior compartment (Figure S2).

Although these lineage tracing experiments demonstrate that the progeny of *Dll*-expressing cells of the VP contribute to dorsal structures, they do not address if the DP requires a contribution from the VP. We first tested this by using Dll^{MD23}-*Gal4* to ablate the ventral progenitor cells by expressing the pro-apoptotic gene *head involution defective* (*hid*). The leg and wing primordia were visualized with *esg-lacZ* (Figure 2A, B and Figure S1C). As expected, no VP cells were observed in these embryos, as seen by the absence of ventral *esg-lacZ* expression. In contrast, DP cells were still present, although the size of dorsal

primordia was reduced by approximately 50% (Figure 2B). Similar results were observed when the dose of the pro-apoptotic genes was increased (Figure 2C–E).

We further tested the independence of the DP by examining embryos mutant for *Dll* and the ventral selector genes *buttonhead* (*btd*) and *Sp1* [23, 34–36]. Even in these triple mutant embryos *sna*-DP and *vg* were normally expressed (Figure 2G). However, although Dll protein is not detected we note that *Dll* ^{MD23}*-Gal4* is still active in the triple mutant, suggesting that VP fates are still partially specified (Figure S2G).

Together, these results suggest that in the absence of the VP, or when the VP is severely compromised, DP fates are still specified, although its size is reduced.

Distinct regulation of the dorsal and ventral primordia

If the DP arise in part independently of the VP, we would expect them to have distinct genetic inputs. However, before carrying out a detailed analysis, we used both gain- and loss-of-function manipulations to demonstrate that *sna*-DP is not a Sna-dependent autoregulatory element, and that it is activated independently of *vg*, presumably by signals and other transcription factors present in these embryos at the correct time and position (Figure S3).

Dll expression in the VP is activated by Wingless (Wg) and restricted dorsally and ventrally by the Decapentaplegic (Dpp) and Epidermal Growth Factor Receptor (EGFR) pathways, respectively [20, 37–39]. We therefore compared how these three pathways influence the formation and size of both primordia, using *sna*-DP-*lacZ* and *Dll* expression as readouts. In addition to examining mutants, as described below we manipulated these pathways in various ways using *prd-Gal4*, which is expressed throughout the T2, but not the T3, segment, thus allowing a comparison of *prd-Gal4* expressing and non-expressing segments in the same embryo (Figure S3).

Wg—Initially, *wg* is expressed in dorso-ventral stripes in the anterior compartment of each thoracic segment that are later interrupted due to repression by the T-box transcription factors encoded by the three *Dorsocross* (*Doc*) genes [40]. Repression of *wg* by Doc creates a Wg free domain in the lateral ectoderm (Figure 3A–C). *sna*-DP activity is only observed after *wg* repression and within the *Doc* expression domain (Figure 3D–F). Consistent with these expression patterns, ectopic activation of the Wg pathway by expressing an activated form of the transcriptional co-activator Armadillo (Arm*) results in a smaller DP and an increase in the number of VP cells (Figure 4C and O). Conversely, downregulation of the Wg pathway using a dominant negative version of the Wg transcriptional effector TCF (TCF^{DN}) had no effect on *sna*-DP, but completely abolished *Dll* expression (Figure 4B and O). Moreover, in embryos homozygous for a deficiency that removes all three *Doc* genes, *Df(3L)DocA,* the DP are absent and there is a dramatic expansion of the *Dll*-expressing VP (Figure 4D and O). Ectopic expression of one of the *Doc* genes, *Doc-2,* eliminates the VP*,* while the number of *sna*-DP positive cells remains unchanged (Figure 4E and O). These data are consistent with the idea that Doc-mediated repression of *wg* is necessary for the formation of the DP, and that *wg* is an essential activator of the VP [20, 39, 41].

Dpp—The dorsal and ventral appendage primordia also have different responses to *dpp*, which is initially expressed as a dorsal spot within *Dll* expressing cells and gradually expands dorsally along with *sna*-1.7 activity (minimized version of *sna*-DP) (Figure 3G–I). The expression of a constitutively active version of the Dpp receptor, $thickveins^{QD}$ (tkv^{QD}) almost doubles the size of the DP without affecting the size of the VP (Figure 4G and O). Inhibition of the Dpp pathway through the expression of the Dpp pathway repressor Brinker (Brk), abolishes both *sna*-DP and *Dll* expression (Figure 4F and O). The effects of Dpp manipulations on *sna*-DP are consistent with previous findings that *dpp* is required for Doc expression [40, 41].

EGFR—Activation of the EGFR pathway, as visualized using an antibody to phospho-MAP Kinase (pMAPK), is initially detected in *Dll* expressing cells at stage 10/11 and by stage 14 is restricted to a subset of the VP and is mostly absent from the DP (Figure 3J–L). Consistent with previous results [38], in *EGFR* mutant embryos the size of the DP increases while the size of the VP is reduced (Figure 4H and O). Conversely, expression of a constitutively active version of the EGFR receptor (*EGFR.λtop*) reduces the size of the DP and increases the size of the VP (Figure 4I and O).

Epistasis experiments—The above experiments suggest that the activation of the *Doc* genes by Dpp results in the repression of *wg* in the lateral ectoderm, thus generating a permissive domain where *sna*-DP can be activated. To further investigate the role of Dpp, Doc and Wg we carried out epistasis experiments to more precisely decipher the logic of *sna*-DP activation.

Initially, we tested if the activation of the Dpp pathway, which increases the size of the DP, would increase their size further when the Wg pathway was downregulated. In $prd>tkv^{QD}$, TCF^{DN} embryos, the size of the DP increased compared to WT (compare Figure 4J with 4A), but was similar to the size observed in $prd>tkv^{QD}$ embryos (compare Figure 4J with 4G and 4O).

We next asked if the *Doc* genes play a role in *sna*-DP activation besides its indirect role through repression of *wg*. First, we tried to rescue the lack of *sna*-DP activation in tkv^{a12} null mutant embryos by expressing *Doc-2* with *prd-Gal4*. Doc-2 was not sufficient to induce *sna*-DP in the absence of *tkv*, suggesting a Doc-independent role for the Dpp pathway in activating *sna*-DP (Figure 4K). Similarly, *sna*-DP expression was not rescued in *Df(3L)DocA* embryos in which the the Wg pathway was downregulated by the expression of TCF^{DN}, suggesting that Doc plays a positive role in addition to repression of *wg* (Figure 4L). In a third experiment, we examined *Df(3L)DocA* embryos in which the Dpp pathway was also upregulated. In these embryos, we observed a small number of *sna*-DP positive cells dorsal to the *Dll* domain (Figure 4M). This limited rescue could be due to ectopic expression of *wg* typical of *Df(3L)DocA* mutant embryos [40]. To test for this, we also downregulated the Wg pathway in these embryos ($Df(3L)DocA; prd>tkv^{QD}, TCF^{DN}$). In these embryos activation of the Dpp pathway was sufficient to increase the number of *sna*-DP expressing cells (Figure 4N).

Together, these epistasis experiments indicate that *sna*-DP is activated by the Dpp pathway by two parallel mechanisms: one is via Dpp's activation of *Doc* (which represses *wg*) and one that is independent of *Doc* (Figure 7). We further conclude that the primary role for *Doc* in the activation of *sna*-DP is to repress *wg*.

Hox regulation of *sna*-DP

Although the Wg, Dpp, and EGFR pathways are deployed similarly in all thoracic and abdominal segments of the embryo, the DP are only formed in the T2 (wing) and T3 (haltere) segments (Figure 1B). Previous results suggest that the Hox proteins control the segmental expression of *Dll* and *vg* [19, 29] and, for *Dll*, direct Hox inputs have been defined that restrict its expression to the three thoracic segments [19, 42, 43]. To investigate the relationship between the Hox genes and the DP, we first compared the expression of the Hox genes *Scr, Antp, Ubx* and *abd-A* with *sna*-DP (Figure 5A–D). At the stage when *sna*-DP is fully activated in T2 and T3 (stage 14), Scr is restricted to the first thoracic segment, T1 (Figure 5A). Antp protein is observed in all three thoracic segments where it overlaps with *sna*-DP at stage 13 (Figure S4). However, by stage 14 Antp is not observed in *sna*-DP positive cells (Figure 5B). In contrast, Ubx overlaps with *sna*-DP in the haltere primordia in T3 but not with the wing primordia in T2 (Figure 5C). Abd-A is restricted to the abdominal segments, with higher levels in the posterior compartment (Figure 5D).

As the regulation of the VP gene *Dll* is compartment specific [43], we examined the relationship between *sna*-DP and the posterior compartment gene *engrailed* (*en*) in WT and Hox mutant embryos. In *Scr* mutant embryos ectopic DP is observed in the T1 segment, in both anterior and posterior compartments (Figure 5F). In *Antp* mutants *sna*-DP is expressed in both compartments, but the number of cells is reduced in T2 (Figure 5G and Q). In *Ubx* mutant embryos, *sna*-DP is derepressed in the anterior compartment of the first abdominal segment (A1) (Figure 5H and Q). Consistent with this observation, in *abd-A* mutant embryos *sna*-DP is derepressed in ~4 posterior compartment cells in abdominal segments (Figure 5I), and in *Ubx abd-A* double mutant embryos *sna*-DP is derepressed in both anterior and posterior compartment cells of the abdominal segments (Figure 5J). In *Ubx* and *Ubx abdA* mutant embryos we also noticed a reduction in the number of *sna*-DP cells in T2 compared to wild type embryos, which may be a consequence of partial derepression of *Scr* (Figure 5Q and Figure S4).

Ectopic expression experiments, using the *prd-Gal4* driver, were also informative (Figure 5K–P). *prd>Scr* is able to nearly eliminate both *sna*-DP and *Dll*, while expressing *abd-A* or *Abd-B* completely eliminates both primordia. In contrast, although *prd>Ubx* fully eliminates the VP, it only reduces the size of the DP. *prd>Antp* did not have any noticeable effect on either Dll or *sna*-DP. Finally, because a portion of the DP is derived from the VP, we considered the possibility that Hox repression of the DP could in part be an indirect consequence of VP repression. However, by using a Gal4 driver that is active in dorsal, but not ventral, regions of each segment, to drive the expression of abdominal Hox proteins, we found that they can repress the DP independently of the VP (Figure S5).

Molecular dissection of *sna*-DP

To address how the signals that regulate the expression of *sna* are integrated at a molecular level we further dissected the *sna*-DP CRM. We reduced the original *sna*-DP to a 1.7 Kb fragment (*sna*-1.7) by comparison to other reporter lines (Figure 1A and Methods). Next, we subdivided the *sna*-1.7 CRM into 4 overlapping fragments (Figure 6A and B). Although the background of *lacZ* increased after minimizing the *sna*-1.7 fragment, the activity in the DP stands out compared to the background. Only the *sna*-1.7-2 fragment reproduced the expression of *sna* in both the anterior and posterior compartments of the dorsal primordia (Figure 6B). *sna*-1.7-3 activity was mostly restricted to the posterior compartment (Figure 6B), but can eventually contribute to both compartments when tested in lineage tracing experiments (Figure S2). Further attempts to dissect *sna*-1.7-2 into smaller subfragments (*sna*-1.7-2A and *sna*-1.7-2.B) were unsuccessful, suggesting that both halves are required for activity (Figure S6). Notably, when in *trans* to an intact *sna*-1.7 reporter inserted into the same chromosomal location, the activity of these subfragments was rescued, most likely by a phenomenon known as transvection [44] (Figure S6).

Because of Dpp's positive role in *sna* activation we searched for binding sites of the transcription factor Mothers against Dpp (Mad) within the minimal *sna*-1.7-2. We found 3 predicted sites that when mutated (*sna*-1.7-2^{Mad}) strongly reduced the levels of the reporter gene expression (Figure 6E and Figure S6). We also identified a site that binds Antp together with the Hox cofactors Extradenticle (Exd) and Homothorax (Hth) that, when mutated, reduced expression (*sna*-1.7-2$^{Hox1\Delta 2}$) (Figure 6F and Figure S7). However, mutation of this or other putative Hox binding sites failed to result in derepression in the abdominal or T1 segments, leaving open the question of whether Hox repression of *sna*-DP in these segments is direct (Figure 6F and G).

Discussion

Here, we describe the first CRM in *Drosophila*, *sna*-DP, that is specifically active in the embryonic progenitors of the wing and haltere imaginal discs. Lineage tracing experiments using this element demonstrate that the embryonic cells marked by *sna*-DP are the progenitors for the entire adult thorax of segments T2 and T3, not just the dorsal appendages (wing and haltere). Thus, by comparing the regulation of *sna*-DP to that of VP-restricted genes and CRMs, we have been able to unambiguously compare the genetic inputs that specify these two primordia, as well as their lineages and spatial relationship to each other. Below we discuss these findings and how they help inform the evolutionary origins of the wing.

Different inputs for specifying the VP and DP

Using *Dll* and a *sna*-DP reporter gene as readouts, we extend previous findings to derive the regulatory inputs into the initial specification of these two primordia [19–21, 29, 37–39, 42, 43]. Our key findings, combined with previous observations, are summarized in Figure 7. In stage 11 embryos, *Dll* is first activated in a group of ~30 cells in each thoracic segment in a Wg-dependent manner. Because these cells can give rise to both ventral and dorsal structures, we refer to this group of cells as the Thoracic Primordia (TP), to highlight the

fact that they have a broader developmental potential compared to the VP, which is defined by the set of *Dll*-expressing cells a few hours later. At this initial stage, the size of the TP is restricted by EGFR ventrally and Dpp dorsally [20, 37]. Also at this early stage, Wg is expressed in a continuous stripe along the dorsal-ventral axis. Soon thereafter, expression of the *Doc* genes is activated in a set of lateral cells in a Dpp-dependent manner [41] and is responsible for repressing *wg*, thus interrupting the Wg stripe [40]. Our experiments demonstrate that both conditions – an absence of Wg and presence of Dpp – are required for the initial expression of *sna*-DP, which is activated in *Dpp*- and *Doc*-expressing and Wg-non-expressing region of the embryo. The identification of essential Mad binding sites suggests that the activation of *sna*-DP by Dpp is direct. In contrast to Dpp-activation of the DP, the primary inducer of *Dll* in the VP is Wg [21, 22, 39]. The role of EGFR signaling is more complex: although it is initially required to restrict *Dll* expression from the ventral midline, this expansion of *Dll* is likely because of a transformation of cell fate [37]. Later in embryogenesis, EGFR signaling plays an activating role in specifying the VP and a negative role in specifying the DP, consistent with previous observations [38].

The TP and, subsequently, the VP are not present in abdominal segments due to repression by the abdominal Hox proteins Ubx and AbdA [19, 42, 43]. There are interesting similarities and differences in the Hox regulation of DP formation. Unlike the VP, which is present in all three thoracic segments, in WT embryos the DP only forms in T2 and T3. Consistently, in *Scr* null embryos *sna*-DP is derepressed in T1. *Antp* has a positive, but not essential role in forming the DP because there are fewer *sna*-DP-expressing cells in *Antp* null embryos. Interestingly, *Antp* has recently been shown to have a positive role in VP size [45]. Further, as observed for *Dll* [43], repression of *sna*-DP by the abdominal Hox proteins occurs in a compartment-specific manner. We also found that a subfragment of *sna*-DP (*sna*-1.7-3) is mostly expressed in the posterior compartment of T2 and T3, suggesting that the compartment-specific repression by Ubx and Abd-A is mediated by distinct inputs into *sna*-DP. However, unlike the regulation of *Dll* in the VP, we have been unable to separate the positive (by Antp) and negative (by Scr, Ubx and Abd-A) Hox inputs into *sna*-DP: when Hox binding sites in *sna*-DP were mutated, we only observed reduced expression, thereby leaving unresolved if Hox-mediated abdominal repression of *sna*-DP is direct. Further, we note that assessing Ubx's role in T3 is not straightforward: while the size of the DP is smaller in T3 compared to T2, in *Ubx* null embryos DP size in T3 does not change. This may in part be because of derepression of *Scr*, which could limit our ability to observe the expected increase in DP size in *Ubx* null embryos. Nevertheless, ectopic expression of *abd-A* in T2 completely eliminates the DP, while ectopic expression of *Ubx* in T2 only reduces the size of DP, highlighting an interesting difference between the activities of these two abdominal Hox proteins.

Implications for the evolution of wings

Our lineage tracing data demonstrate that the wing and haltere imaginal discs are derived from two populations of cells: those that originate in the TP (marked by activity of the early *Dll* CRM, *Dll304*), and those that receive distinct cues (high Dpp, low Wg) in more dorsal positions of the thoracic segments. Although these lineage tracing experiments suggest that both populations of cells have the potential to give rise to any part of the wing and haltere

imaginal discs, we highlight two differences. First, lineage tracing using TP drivers labels only a portion of each wing disc, and the labeled cells have a tendency to be in the ventral portion of the disc. The ventral bias may be a consequence of the ventral position of the TP relative to the DP, suggesting that the fate of these cells is due to their relative position in the embryo. In contrast, lineage tracing performed with *sna*-DP is 100% efficient, consistently labeling the entire wing and haltere imaginal discs. The complete labeling of these discs by *sna*-1.7 argues that the cells that express that CRM, which include the cells derived from the TP, are the precursors of the entire dorsal thorax.

We suggest that the dual developmental origins of the wing primordia may be a molecular remnant of the evolutionary history of this appendage and thus support a dual evolutionary origin of the wing. Interestingly, this idea has also been suggested based on recent expression studies of wing marker genes [3, 14, 15], functional approaches [16, 17] and fossil analysis [18]. In future work, it will be interesting to investigate whether similar CRMs with *sna*-DP-like activity are conserved in other organisms such as crustaceans. Interestingly, and consistent with this notion, it is noteworthy that a *sna* ortholog is expressed adjacent to the limb buds in the crustacean *Parhyale hawaiensis* [46].

In summary, by carrying out CRM-based lineage analyses and genetic studies, our observations complement comparative expression approaches and provide additional support for a dual origin model of the dorsal appendages. From an evolutionary point of view, there are two advantages of such a model. For one, the dorsal contribution to the wing could have provided an initial wing-like structure that allowed airborne insects to glide. Second, a ventral/coxa contribution could have provided an initial source of muscles innervated by motor neurons, allowing directed movements of this structure. It is particularly striking that the dual origins of the DP are still observable in a dipteran fly such as *Drosophila*, which unlike crustaceans undergoes holometabolan development where the adult structures develop from cells set aside early in embryogenesis. If the dual specification of the dorsal appendage occurs in both holo- and hemimetabolan insects, it would support the idea that it predates the origin of holometabolous metamorphosis.

STAR Methods

Contact for reagents and resource sharing

Further information and requests for resources and reagents should be directed to and will be fulfilled by the Lead Contact, Carlos Estella (cestella@cbm.csic.es).

Experimental model and subject details

Fly and embryo culture: *Drosophila melanogaster* were maintained at 25°C on standard cornmeal agar diet in a humidified incubator. Embryos were collected in apple juice agar plates for 12 hrs. Fly strains are provided in the key resources table.

Fly stocks—*prd-Gal4*, esg^{NP5130}*-Gal4*, Dll^{MD23}*-Gal4*, *Dll304-Gal4*, $tubGal80^{ts}$, *Doc-1-Gal4* (GMR 45H05), esg^{05730}*-lacZ* and dpp^{10638}*-lacZ* are all described in Flybase and key resource table. For lineage trace analyses the *act5C>stop>lacZ*; UAS-*flp* [47] stock was crossed with the corresponding *Gal4* lines. For *Dll* lineage analysis, we restricted the activity

of the *Dll*^{MD23}*-Gal4* line to embryogenesis using the *tubGal80*^{ts}. Briefly, embryos were collected at 25° for 12hrs, transferred to 29° for 24hrs and then to 17° until dissection to shutdown Gal4 activity.

Scr^{4}, *Antp25*, *Ubx*^{Mx12}*abd-A*^{M1}, *Df(btd,Sp1)*, *Df(3l)DocA*, *EGFR*^{null}, *tkv*^{a12}, *Dll*^{SA1}, *vg*^{null} and *sna*^{V2} are described in Flybase. UAS-*hid*, UAS-*rpr*, UAS-*GFP*, 20XUAS-6X*GFP*, UAS-*TCF*^{DN}, UAS-*arm** (delta N), UAS-*brk*, UAS-*tkv*^{QD}, UAS-*TCF*^{DN}, UAS-*Doc-2*, UAS-*EGFRλtop4.2*, UAS-*Scr*, UAS-*Antp*, UAS-*Ubx*, UAS-*abd-A*, UAS-*Abd-B*, UAS-*vg*, UAS-*sna* are described in Flybase and key resource table.

Method Details

Immunofluorescence—Imaginal discs were dissected in PBS and fixed with 4% paraformaldehyde in PBS for 25 minutes at room temperature. They were blocked in PBS, 1% BSA, 0.3% Triton for 1 hour, incubated with the primary antibody over night at 4°C, washed four times in blocking buffer, and incubated with the appropriate fluorescent secondary antibody for 1 hour at room temperature in the dark. They were then washed and mounted in Vectashield (Vector Laboratories). Embryos were collected every 12 hrs and dechorionated in 100% bleach for 3 minutes and fixed in 1X PBS, 4% formaldehyde and heptane solution for 25 minutes. Then embryos were devitellinized with methanol and wahsed in PBT (1X PBS and 0.1% tween 20). Embryos were blocked in 3% BSA PBT for 1 hour and incubated with primary antibodies over night, washed four times in PBT, and incubated with the appropriate fluorescent secondary antibody for 1 hour at room temperature in the dark. They were then washed and mounted in Vectashield.

Confocal images were obatined with a Zeiss LSM510 coupled to a vertical Axio Imager.Z1 M.

For visualization a Z-projection was generated using Image J (https://imagej.nih.gov/ij/) for representative embryos of each stage and genotype.

Generation of transgenes—*sna*-DP, *sna*-1.7, *sna*-1.7-1, *sna*-1.7-2, *sna*-1.7-3 and *sna*-1.7-4 sequences were cloned into the attB-hs43-nuc-lacZ plasmid vector [22]. *sna*-1.7 and *sna*-1.7-3 were also cloned in the pBPGUw (Gal4) vector [48]. The primers used for cloning each reporter line are described in the key resources table.

Putative Mad and Hox binding sites were identified on the basis of a bioinformatics analysis combining data from the JASPAR CORE Insecta database (http://jaspar.genereg.net/) and the Target Explorer tool [49]. Mutagenesis of the Mad and Hox putative binding sites was performed using the QuikChange Site-Directed Mutagenesis Kit (Stratagene). The primers used for the mutagenesis are described in in the key resources table. All reporter constructs were inserted in the same site 3R (86Fb) to allow proper comparisons. In addition, *sna*-DP-*lacZ* and *sna*-1.7-*Gal4* were also inserted in 2R (51D).

Electrophoretic mobility shift assays (EMSAs)—Binding experiments were performed as described previously [42]. Proteins were expressed as His-tag fusions and purified from BL21 cells. HM protein (HM refer to the full-length homeodomainless

isoform of Hth) was purified in complex with Exd. Binding reactions for Dfd, Ubx, and AbdA were performed with 150nM Hox protein and 75nM Exd/HM. Antp protein was used at a concentration of 75nM with 30nM Exd/HM. DNA probes were radiolabeled with P32 and used at a concentration of 6nM in the binding reaction.

Quantification and Statistical Analysis

sna-DP and Dll positive cells were counted by taking multiple Z stacks to encompass the entire primordia using Image J (https://imagej.nih.gov/ij/). At least 10 embryos were counted per genotype. Statistical analysis, * $p<0.05$ with Student's t-test. Error bars represent the standard error of the mean.

Supplementary Material

Refer to Web version on PubMed Central for supplementary material.

Acknowledgments

We thank Ingolf Reim, Ernesto Sánchez-Herrero and Fernando Diaz-Benjumea for fly stocks and reagents. We thank Richard Allan for his initial contributions to the project and Nuria Esteban for technical help. We also thank Ernesto Sánchez-Herrero, Molly Przeworski, and members of the Mann and Estella labs for comments on the manuscript. This study was supported by grants from the Secretaría de Estado de Investigación, Desarrollo e Innovación (Ministerio de Economía y Competitividad) [No. BFU2015-65728-P to C.E.] and NIH grants RO1GM058575 and R35GM118336 awarded to R.S.M.

References

1. Engel MS. Insect evolution. Current biology : CB. 2015; 25:R868–872. [PubMed: 26439349]
2. Grimaldi, D., Engel, M. Evolution of the Insects. Cambridge University Press; 2005.
3. Clark-Hachtel CM, Tomoyasu Y. Exploring the origin of insect wings from an evo-devo perspective. Curr Opin Insect Sci. 2016; 13:77–85. [PubMed: 27436556]
4. Snodgrass, RE. Principles of insect morphology. New York: McGraw Hill; 1935. p. 667
5. Crampton G. The phylogenetic origin and the nature of the wings of insects according to the paranotal theory. Journal of the New York Entomological Society. 1916; 24:1–39.
6. Kukalova-Peck J. Origin of the insect wing and wing articulation from the arthropodan leg. Canadian Journal of Zoology. 1983; 61:1618–1669.
7. Kukalova-Peck J. Origin and evolution of insect wings and their relation to metamorphosis, as documented by the fossil record. Journal of Morphology. 1978; 156:53–125.
8. Averof M, Cohen SM. Evolutionary origin of insect wings from ancestral gills. Nature. 1997; 385:627–630. [PubMed: 9024659]
9. Wigglesworth V. Evolution of Insect Wings and Flight. Nature. 1973; 246:127–129.
10. Coulcher JF, Edgecombe GD, Telford MJ. Molecular developmental evidence for a subcoxal origin of pleurites in insects and identity of the subcoxa in the gnathal appendages. Sci Rep. 2015; 5:15757. [PubMed: 26507752]
11. Rasnitsyn A. A modified paranotal theory of insect wing origin. Journal of morphology. 1981; 168:331–338.
12. Damen WG, Saridaki T, Averof M. Diverse adaptations of an ancestral gill: a common evolutionary origin for wings, breathing organs, and spinnerets. Current biology : CB. 2002; 12:1711–1716. [PubMed: 12361577]
13. Jockusch EL, Nagy LM. Insect evolution: how did insect wings originate? Current biology : CB. 1997; 7:R358–361. [PubMed: 9197228]
14. Clark-Hachtel CM, Linz DM, Tomoyasu Y. Insights into insect wing origin provided by functional analysis of vestigial in the red flour beetle, Tribolium castaneum. Proceedings of the National

Academy of Sciences of the United States of America. 2013; 110:16951–16956. [PubMed: 24085843]

15. Niwa N, Akimoto-Kato A, Niimi T, Tojo K, Machida R, Hayashi S. Evolutionary origin of the insect wing via integration of two developmental modules. Evol Dev. 2010; 12:168–176. [PubMed: 20433457]
16. Elias-Neto M, Belles X. Tergal and pleural structures contribute to the formation of ectopic prothoracic wings in cockroaches. R Soc Open Sci. 2016; 3:160347. [PubMed: 27853616]
17. Medved V, Marden JH, Fescemyer HW, Der JP, Liu J, Mahfooz N, Popadic A. Origin and diversification of wings: Insights from a neopteran insect. Proceedings of the National Academy of Sciences of the United States of America. 2015; 112:15946–15951. [PubMed: 26668365]
18. Prokop J, Pecharova M, Nel A, Hornschemeyer T, Krzeminska E, Krzeminski W, Engel MS. Paleozoic Nymphal Wing Pads Support Dual Model of Insect Wing Origins. Current biology : CB. 2017; 27:263–269. [PubMed: 28089512]
19. Vachon G, Cohen B, Pfeifle C, McGuffin ME, Botas J, Cohen SM. Homeotic genes of the Bithorax complex repress limb development in the abdomen of the Drosophila embryo through the target gene Distal-less. Cell. 1992; 71:437–450. [PubMed: 1358457]
20. Cohen B, Simcox AA, Cohen SM. Allocation of the thoracic imaginal primordia in the Drosophila embryo. Development. 1993; 117:597–608. [PubMed: 8330530]
21. McKay DJ, Estella C, Mann RS. The origins of the Drosophila leg revealed by the cis-regulatory architecture of the Distalless gene. Development. 2009; 136:61–71. [PubMed: 19036798]
22. Estella C, McKay DJ, Mann RS. Molecular integration of wingless, decapentaplegic, and autoregulatory inputs into Distalless during Drosophila leg development. Developmental cell. 2008; 14:86–96. [PubMed: 18194655]
23. Estella C, Voutev R, Mann RS. A dynamic network of morphogens and transcription factors patterns the fly leg. Current topics in developmental biology. 2012; 98:173–198. [PubMed: 22305163]
24. Whiteley M, Noguchi PD, Sensabaugh SM, Odenwald WF, Kassis JA. The Drosophila gene escargot encodes a zinc finger motif found in snail-related genes. Mechanisms of development. 1992; 36:117–127. [PubMed: 1571289]
25. Hayashi S, Hirose S, Metcalfe T, Shirras AD. Control of imaginal cell development by the escargot gene of Drosophila. Development. 1993; 118:105–115. [PubMed: 8375329]
26. Alberga A, Boulay JL, Kempe E, Dennefeld C, Haenlin M. The snail gene required for mesoderm formation in Drosophila is expressed dynamically in derivatives of all three germ layers. Development. 1991; 111:983–992. [PubMed: 1879366]
27. Fuse N, Hirose S, Hayashi S. Determination of wing cell fate by the escargot and snail genes in Drosophila. Development. 1996; 122:1059–1067. [PubMed: 8620833]
28. Williams JA, Bell JB, Carroll SB. Control of Drosophila wing and haltere development by the nuclear vestigial gene product. Genes & development. 1991; 5:2481–2495. [PubMed: 1752439]
29. Carroll SB, Weatherbee SD, Langeland JA. Homeotic genes and the regulation and evolution of insect wing number. Nature. 1995; 375:58–61. [PubMed: 7723843]
30. Ip YT, Park RE, Kosman D, Yazdanbakhsh K, Levine M. dorsal-twist interactions establish snail expression in the presumptive mesoderm of the Drosophila embryo. Genes & development. 1992; 6:1518–1530. [PubMed: 1644293]
31. Ip YT, Levine M, Bier E. Neurogenic expression of snail is controlled by separable CNS and PNS promoter elements. Development. 1994; 120:199–207. [PubMed: 8119127]
32. Dunipace L, Ozdemir A, Stathopoulos A. Complex interactions between cis-regulatory modules in native conformation are critical for Drosophila snail expression. Development. 2011; 138:4075–4084. [PubMed: 21813571]
33. Wieschaus E, Gehring W. Clonal analysis of primordial disc cells in the early embryo of Drosophila melanogaster. Developmental biology. 1976; 50:249–263. [PubMed: 819316]
34. Cordoba S, Requena D, Jory A, Saiz A, Estella C. The evolutionarily conserved transcription factor Sp1 controls appendage growth through Notch signaling. Development. 2016; 143:3623–3631. [PubMed: 27578786]

35. Estella C, Mann RS. Non-redundant selector and growth-promoting functions of two sister genes, buttonhead and Sp1, in Drosophila leg development. PLoS genetics. 2010; 6:e1001001. [PubMed: 20585625]
36. Estella C, Rieckhof G, Calleja M, Morata G. The role of buttonhead and Sp1 in the development of the ventral imaginal discs of Drosophila. Development. 2003; 130:5929–5941. [PubMed: 14561634]
37. Goto S, Hayashi S. Specification of the embryonic limb primordium by graded activity of Decapentaplegic. Development. 1997; 124:125–132. [PubMed: 9006073]
38. Kubota K, Goto S, Eto K, Hayashi S. EGF receptor attenuates Dpp signaling and helps to distinguish the wing and leg cell fates in Drosophila. Development. 2000; 127:3769–3776. [PubMed: 10934021]
39. Kubota K, Goto S, Hayashi S. The role of Wg signaling in the patterning of embryonic leg primordium in Drosophila. Developmental biology. 2003; 257:117–126. [PubMed: 12710961]
40. Reim I, Lee HH, Frasch M. The T-box-encoding Dorsocross genes function in amnioserosa development and the patterning of the dorsolateral germ band downstream of Dpp. Development. 2003; 130:3187–3204. [PubMed: 12783790]
41. Hamaguchi T, Yabe S, Uchiyama H, Murakami R. Drosophila Tbx6-related gene, Dorsocross, mediates high levels of Dpp and Scw signal required for the development of amnioserosa and wing disc primordium. Developmental biology. 2004; 265:355–368. [PubMed: 14732398]
42. Gebelein B, Culi J, Ryoo HD, Zhang W, Mann RS. Specificity of Distalless repression and limb primordia development by abdominal Hox proteins. Developmental cell. 2002; 3:487–498. [PubMed: 12408801]
43. Gebelein B, McKay DJ, Mann RS. Direct integration of Hox and segmentation gene inputs during Drosophila development. Nature. 2004; 431:653–659. [PubMed: 15470419]
44. Duncan IW. Transvection effects in Drosophila. Annual review of genetics. 2002; 36:521–556.
45. Uhl JD, Zandvakili A, Gebelein B. A Hox Transcription Factor Collective Binds a Highly Conserved Distal-less cis-Regulatory Module to Generate Robust Transcriptional Outcomes. PLoS genetics. 2016; 12:e1005981. [PubMed: 27058369]
46. Hannibal RL, Price AL, Parchem RJ, Patel NH. Analysis of snail genes in the crustacean Parhyale hawaiensis: insight into snail gene family evolution. Development genes and evolution. 2012; 222:139–151. [PubMed: 22466422]
47. Struhl G, Basler K. Organizing activity of wingless protein in Drosophila. Cell. 1993; 72:527–540. [PubMed: 8440019]
48. Pfeiffer BD, Jenett A, Hammonds AS, Ngo TT, Misra S, Murphy C, Scully A, Carlson JW, Wan KH, Laverty TR, et al. Tools for neuroanatomy and neurogenetics in Drosophila. Proceedings of the National Academy of Sciences of the United States of America. 2008; 105:9715–9720. [PubMed: 18621688]
49. Sosinsky A, Bonin CP, Mann RS, Honig B. Target Explorer: An automated tool for the identification of new target genes for a specified set of transcription factors. Nucleic acids research. 2003; 31:3589–3592. [PubMed: 12824372]

Highlights

- An enhancer that marks the initial wing primordia in *Drosophila* is defined
- The signals that initiate wing and leg development are distinct
- Lineage experiments show the wing comes from ventral and dorsal primordia
- Insect wings may have evolved from dual ventral and dorsal inputs

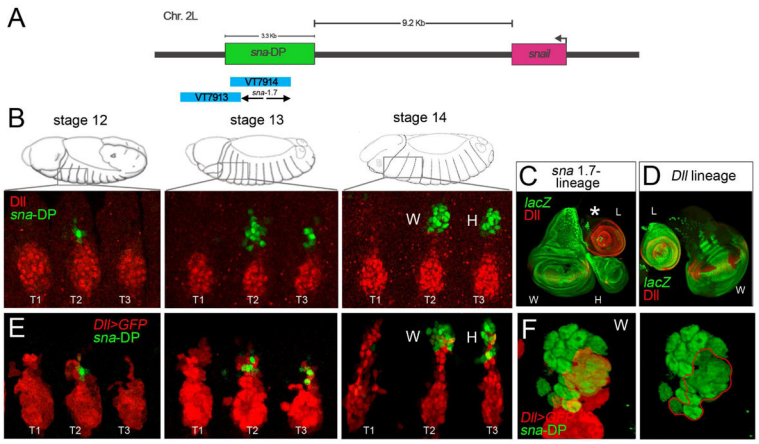

Figure 1. Overview of the *sna*-DP enhancer and its relationship to *Dll* expression

(A) The *sna* genomic region. *sna*-DP CRM (green bar) is a 3.3 kb fragment 3′ to the *sna* transcription start site. VT7914, but not VT7913, (both from VDRC) is active in the DP, and *sna*-1.7 is defined by the non-overlapping region of these two fragments.

(B) Embryonic time course of *sna*-DP activity (green) compared to Dll protein (red).

(C, D) Lineage tracing results for *sna*-DP (C) and *Dll* (D). (C) The progeny of *sna*-DP cells (green) label the entire wing and haltere imaginal discs and a small number of cells in the leg (asterisk). (D) The progeny of *Dll* expressing cells (green) contribute to the entire leg and to parts of the wing disc (see also Figure S2).

(E, F) Time course of *sna*-DP activity (driving nuclear *lacZ;* green) compared to *Dll>GFP* (red). Note that some cells derived from the VP (due to perdurance of GFP from *Dll>GFP*; red) overlap with *sna*-DP expressing DP cells (green). (F) An enlargement of a stage 14 wing primordia. W, wing primordia. H, haltere primordia. L, leg primordia. See also Figures S1 and S2 and Movie S1.

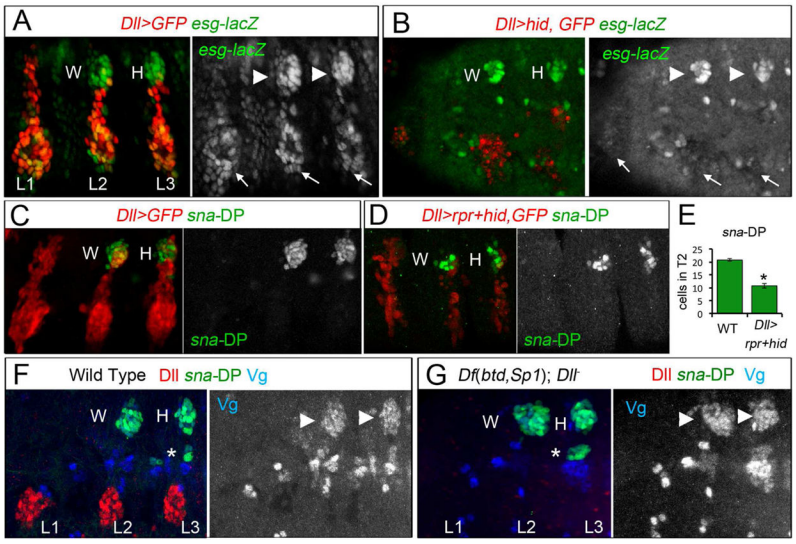

Figure 2. The DP is reduced when the VP is ablated

(A) Thoracic view of *esg-lacZ* (green) and *Dll>GFP* (red) expression in wild type stage 14 embryos. The three leg and DP are labeled with arrows and arrowheads, respectively.

(B) Genetic ablation of the ventral primordia in *Dll>hid* embryos (red and arrows) reduced the size of the DP (arrowheads) and eliminates ventral expression of *esg-lacZ,* (arrows).

(C) Thoracic view of *sna*-DP (green) and *Dll>GFP* (red) in wild type stage 14 embryo.

(D) Ablation of the ventral primordia in *Dll>rpr+hid* embryos (red and arrows) reduced the size of the DP (green).

(E) Quantification of the number in T2 of *sna*-DP (green bars) in wild type and *Dll>rpr+hid* enbryos. * $p<0.05$ with Student's t-test.

(F) Wild type stage 14 embryo stained for *sna*-DP-*lacZ* (green), Vg (blue) and Dll (red).

(G) A stage 14 *Df(btd,Sp1); Dll*$^{-}$ embryo. DP size is unaffected. An asterisk (*) in F and G label a band of muscle cells that express *sna*-DP and Vg. See also Figure S2.

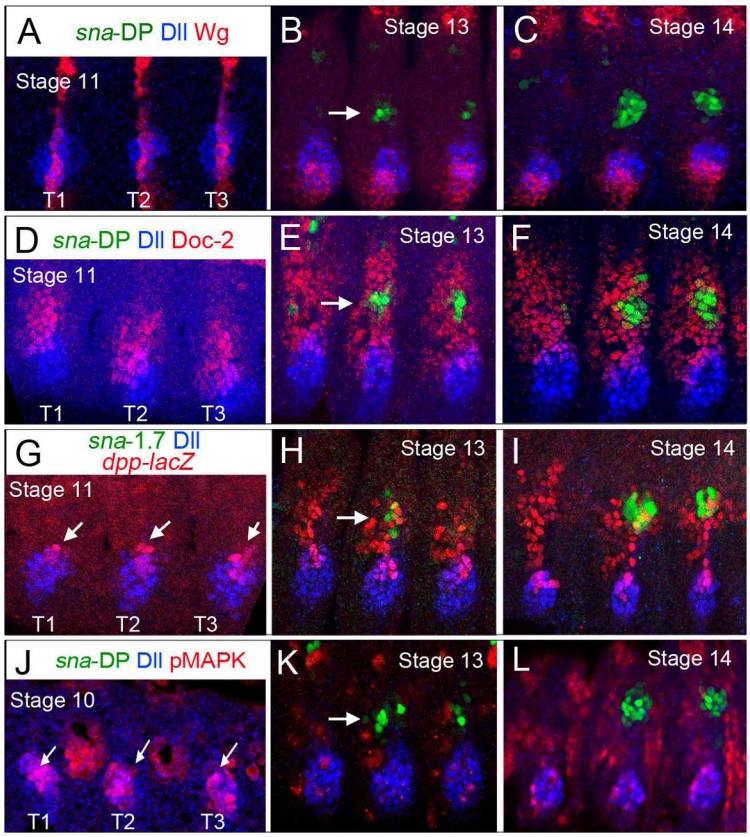

Figure 3. Relationship between *sna*-DP, Dll, Doc, and signaling pathways

All panels show thoracic views of wild type embryos stained for the indicated markers.

(A–C) At stage 11 Wg is expressed in uninterrupted dorso-ventral stripes. Later *sna*-DP is activated in a lateral domain where the Wg stripe is interrupted (arrow).

(D–F) *sna*-DP is activated within the Doc-2 domain (arrow). (G–I) *dpp* is initially expressed as a dorsal spot within *Dll* expressing cells (arrows). At stage 13 and 14 *sna*-DP is activated in *dpp-lacZ* expressing cells.

(J–L) pMAPK is detected within *Dll* expressing cells at stage 10 (arrows in J). *sna*-DP is active in cells with low or no pMAPK staining. See also Figures S3.

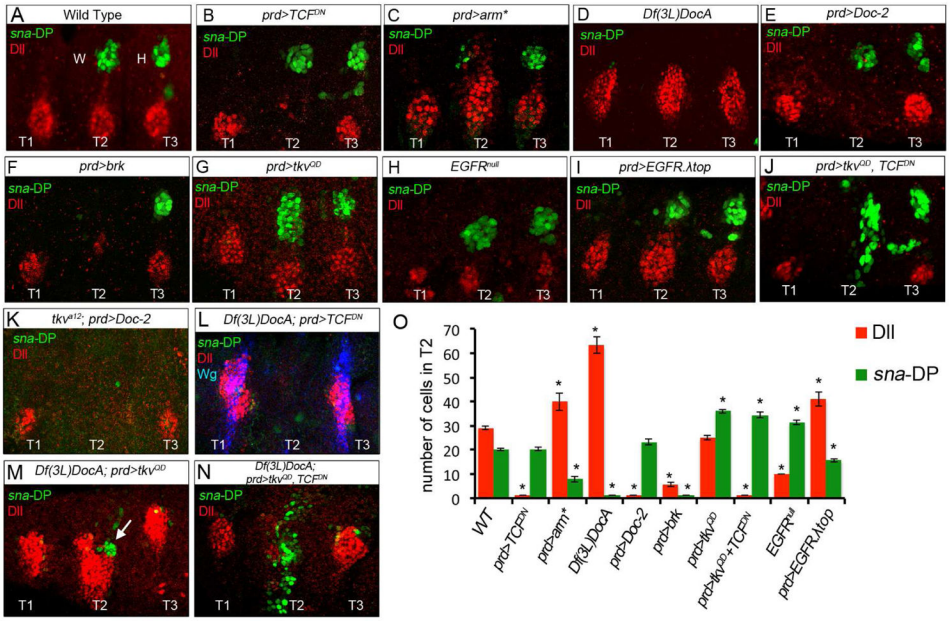

Figure 4. Distinct regulation of *Dll* and *sna*-DP

Thoracic regions of stage 14 embryos stained for Dll (red) to mark the VP, *sna*-DP (green) to mark the DP, and Wg (L, blue).

(A) Wild type.

(B) In *prd>TCF^DN* embryos the VP is absent and DP not affected in T2.

(C) In *prd>arm** embryos VP size increases and DP size decreases in T2.

(D) In *Df(3L)DocA* embryos DP is absent and VP size is doubled.

(E) In *prd>Doc-2* embyros, VP is absent and DP size is unchanged.

(F) In *prd>brk* embryos both the VP and DP are absent in T2.

(G) In *prd>tkv^QD* embryos DP size increases, while VP size is unchanged in T2.

(H) In *EGFR^null* mutant embryos, VP size is reduced and DP size increases.

(I) In *prd>EGFR.* top VP size increases and DP size is reduced in T2.

(J) In *prd>tkv^QD, TCF^DN* embryos DP size increases and shifts them ventrally. VP are absent.

(K) A *tkv^a12, prd>Doc-2* embryo. Without Dpp signaling, resupplying Doc-2 does not rescue DP formation.

(L) A *Df(3L)DocA, prd>TCF^DN* embryo. Reducing Wg pathway activation in the absence of the *Doc* genes fails to rescue DP formation. *Dll* and *wg* expression are absent in T2.

(M) A *Df(3L)DocA, prd>tkv^QD* embryo. Increasing Dpp pathway activity partially rescues DP formation (arrow).

(N) A *Df(3L)DocA; prd>tkv^QD, TCF^DN* embryo. Simultaneously activating the Dpp pathway and repressing the Wg pathway in the absence of the *Doc* genes further increases DP size (compare with M).

(O) Quantification of DP (green bars) and VP (red bars) size in the genetic backgrounds shown in (A–J). * p<0.05 with Student's t-test indicates a significant difference from wild type T2.

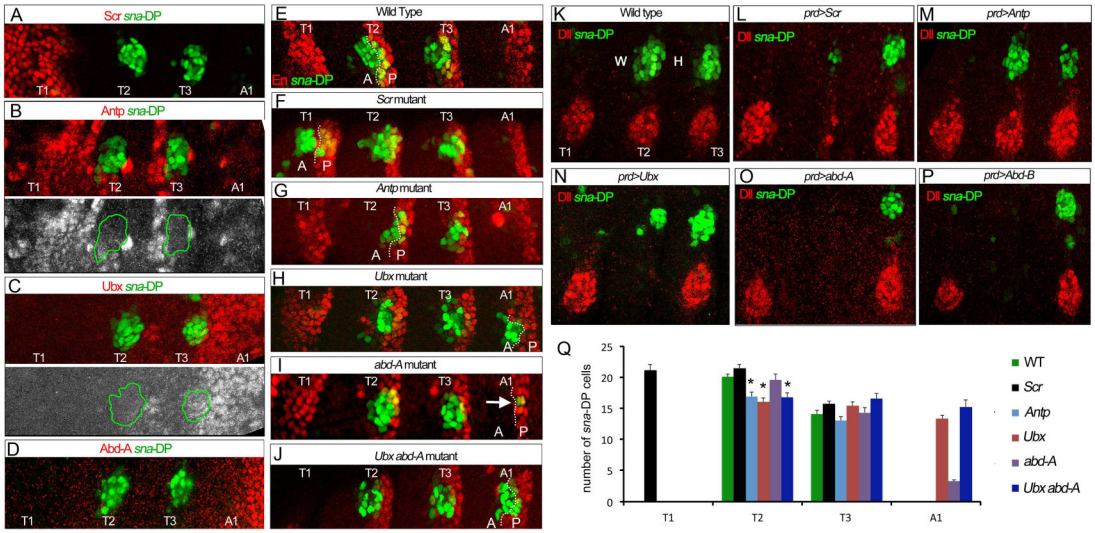

Figure 5. Hox regulation of *sna*-DP

(A–D) Thoracic and first abdominal segments of stage 14 embryos stained for *sna*-DP (green) and Scr (red), Antp (red or white in B), Ubx (red or white in C) and Abd-A (red in D). The wing and haltere primordia are outlined in green.

(E–J) Thoracic and first abdominal segments of stage 14 embryos stained for *sna*-DP (green) and En (red) in wild type (E), *Scr* (F), *Antp* (G), *Ubx* (H), *abd-A* (I) and *Ubx abd-A* double (J) mutant embryos. The anterior (A) –posterior (P) compartment border is indicated with a dotted line. Arrow in (H) points to *sna*-DP cells in the P compartment of A1 in *abdA* mutant embryos.

(K–P) Thoracic segments of stage 14 embryos stained for *sna*-DP (green) and Dll (red) in wild type (K), *prd>Scr* (L), *prd>Antp* (M), *prd>Ubx* (N), *prd>abd-A* (O) and *prd>Abd-B* (P) embryos. Ectopic expression of *Scr*, *abd-A* or *Abd-B* in T2 represses *Dll* and *sna*-DP while *prd>Antp* does not change these readouts. *prd>Ubx* reduces the size of the DP domain and eliminates *Dll*.

(Q) Quantification of DP size in T2 in Hox mutant genotypes. * $p<0.05$ with Student's t-test indicates a significant difference from wild type T2. See also Figures S4 and S5.

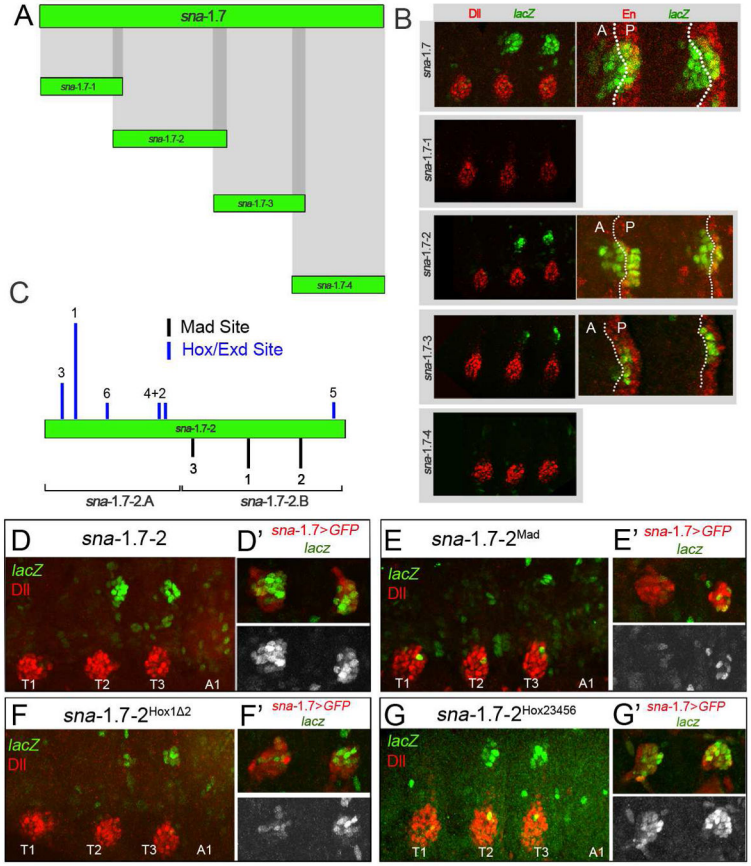

Figure 6. Molecular dissection of *sna*-DP

(A) Division of *sna*-1.7 into 4 overlapping fragments.

(B) Thoracic segments of stage 14 embryos stained for Dll or En (red) and βgal (green). *sna*-1.7 reproduces the activity of *sna*-DP in both the A and P compartments. *sna*-1.7-2 is active in both compartments, while *sna*-1.7-3 is mostly restricted to the P compartment. *sna*-1.7-1 and *sna*-1.7-4 do not drive any expression in the DP.

(C) *sna*-1.7-2 has predicted binding sites for Hox/Exd (blue lines) and Mad (black lines). The height of the bar indicates the relative score (JASPAR). Subfragments *sna*-1.7-2.A and *sna*-1.7-2.B are indicated.

(D–G) Thoracic and first abdominal segments of stage 14 embryos stained for Dll (red) and βgal (green). The right panels show the DP region where the activity of *sna*-1.7>*GFP* (red) is compared to the activity of mutant *sna*-1.7-2 elements (green or white). (D) *sna*-1.7-2.

(E) *sna*-1.7-2^{Mad} with the three predicted Mad sites mutated.

(F) *sna*-1.7-2$^{Hox1\Delta2}$ with Hox site 1 mutated. (G) *sna*-1.7-2^{Hox23456} with Hox sites 2–6 mutated. See also Figures S6 and S7.

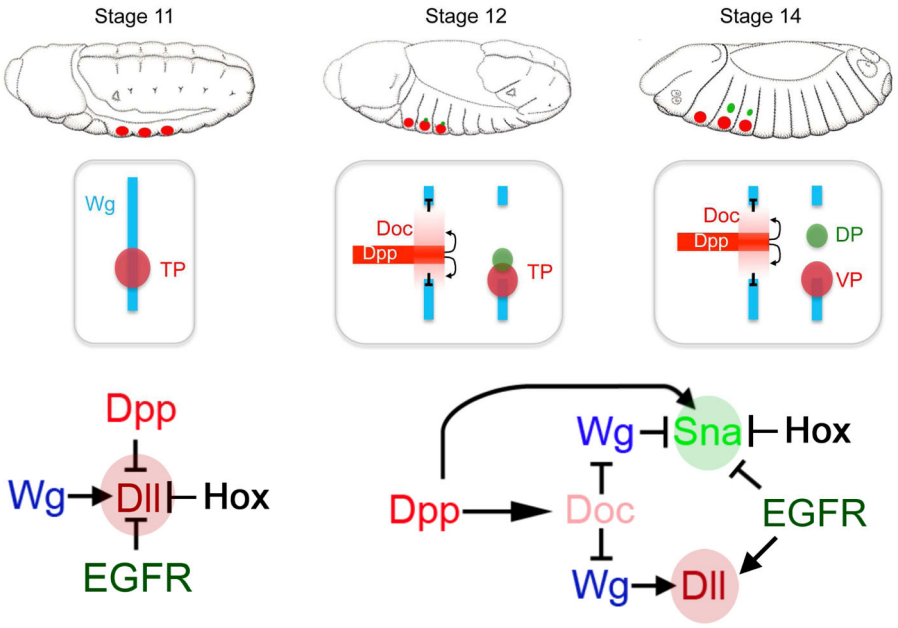

Figure 7. Origin and specification of the *Drosophila* wing

At stage 11, *wg* is expressed in continuous dorso-ventral stripes in each segment of the embryo. As the initial group of *Dll* expressing cells (red circles) contributes to both the DP and VP we refer to them as thoracic primordia (TP). By stage 12, *Doc* is activated by Dpp and represses *wg* in the lateral ectoderm. The dorsal primordia (DP, green circle) originates from two populations of cells: one within the TP (cells that had previously expressed *Dll*) and a second group dorsal to the TP. As embryogenesis progresses the DP separates from the VP. The bottom panels show the known inputs into *Dll* and *sna*-DP when *Dll* is first activated (left) and when *sna*-DP is activated (right).

KEY RESOURCES TABLE

REAGENT or RESOURCE	SOURCE	IDENTIFIER
Antibodies		
Rabbit anti-β-Gal	MP	559761
Mouse anti-β-Gal	Promega	Z378A
Rabbit anti-GFP	ThermoFisher	A6455
Mouse anti-Wg	DSHB	4D4
Mouse anti-En	DSHB	4D9
Mouse anti-Scr	DSHB	6H4.1
Mouse anti-Ubx	DSHB	FP3.38
Mouse anti-Antp	DSHB	4C3
Rabbit anti-Abd-A	Santa Cruz	d-130
Guinea Pig-anti-Sna	gift from Yutaka Nibu, Cornell University, USA	
Rabbit anti-Vg	gift of Sean Carroll University of Wisconsin-Madison, USA	
Guinea Pig anti-Dll	[19]	
Guinea Pig anti-Hth	[19]	
Rabbit anti-Doc-2	gift from Ingof Reim, Friedrich-Alexander University Erlangen-Nürnberg, Germany	
Rabbit anti-Phospho-p44/42 MAPK	Cell Signaling	9101
Experimental Models: Organisms/Strains		
prd-Gal4	Flybase	FBtp0000358
esg^{NP5130}-Gal4	Flybase	FBal0098823
Dll^{MD23}-Gal4	Flybase	FBti0002783
Doc-1-Gal4 (GMR 45H05)	Flybase	FBsf0000164776
Dll304-Gal4	Flybase	FBal0288749
esg^{05730}-lacZ	Flybase	FBti0008070
dpp^{10638} -lacZ	Flybase	FBti0002737
act5C>stop>lacZ; UAS-*flp*	[46]	
Scr^{4}	Flybase	FBal0015280
Antp^{25}	Flybase	FBal0000566
Ubx^{1}	Flybase	FBal0017338
Ubx^{Mx12}abd-A^{M1}	Gift from Ernesto Sanchez-Herrero	
Df(btd,Sp1)	Flybase	FBab0047246
EGFR^{null}	Flybase	FBal0066102
Df(3l)DocA	Flybase	FBab0037663
tkv^{a12}	Flybase	FBal0016821
vg^{null}	Flybase	FBal0093753

REAGENT or RESOURCE	SOURCE	IDENTIFIER
sna^{V2}	Flybase	FBal0015896
UAS-*rpr*	Flybase	FBst0005823
UAS-*hid*	Flybase	FBtp0012437
UAS-*GFP*	Flybase	FBti0012493
UAS-*TCF*^{DN}	Flybase	FBtp0001721
UAS-*arm** (delta N)	Flybase	FBtp0001725
UAS-*brk*	Flybase	FBtp0085350
UAS-*tkv*^{QD}	Flybase	FBtp0001199
UAS-*Doc-2*	Flybase	FBtp0017741
UAS-*EGFRλtop4.2*	Flybase	FBtp0008722
UAS-*Scr*	Flybase	FBtp0000719
UAS-*Antp*	Flybase	FBtp0014554
UAS-*Ubx*	Flybase	FBal0039098
UAS-*abd-A*	Flybase	FBtp0085557
UAS-*Abd-B*	Flybase	FBal0038086
UAS-*vg*	Flybase	FBtp0051400
UAS-*sna*	Flybase	FBtp0009053
Recombinant Proteins		
His-tag HM (Hth)	[40]	
His-tag Exd	[40]	
His-tag Dfd	[40]	
His-tag Antp	[40]	
His-tag Ubx	[40]	
His-tag Abd-A	[40]	
Oligonucleotides		
sna-DP sense: cagtAAGCTTgtggagcgcaccccaaagct		
sna-DP asense: cagtAGATCTaagggatctgataaagaacgatctcc		
sna-1.7 sense: cagtAAGCTTggttggggttaaagtagagcggc		
sna-1.7 asense: cagtAGATCTtggcaaccgactaacaacgcatc		
sna-1.7-1 sense: cagtAAGCTTggttggggttaaagtagagc		
sna-1.7-1 asense: cagtAGATCTttgatcttgcgggtaagccc		
sna-1.7-2 sense: cagtAAGCTTttcttatgggcttacccgca		
sna-1.7-2 asense: cagtAGATCTcaaagctcagcagcggcagc		
sna-1.7-3 sense: cagtAAGCTTgctgccgctgctgagctttg		
sna-1.7-3 asense: cagtAGATCTatacgttaggcattgctatc		
sna-1.7-4 sense: cagtAAGCTTtagcaatgcctaacgtatcg		
sna-1.7-4 asense: cagtAGATCTtggcaaccgactaacaacgc		
sna-1.7-2A sense: cagtAAGCTTttcttatgggcttacccgca		
sna-1.7-2A asense: cagtAGATCTggtaggaataaaccggaggag		

REAGENT or RESOURCE	SOURCE	IDENTIFIER
sna-1.7-2B sense: cagtAAGCTTgaatggcgcccgcctcgattt		
sna-1.7-2B asense: cagtAGATCTcaaagctcagcagcggcagc		
sna-1.7 sense pEntry: CACCggttggggttaaagtagagcggc		
sna-1.7-2 sense pEntry: CACCttcttatgggcttacccgca		
sna-1.7-3 sense pEntry: CACCgctgccgctgctgagctttg		
Mad-1 sense: gtccgccattaaacgatATCATAAtgtTAATtatgtttacagatttgtcg		
Mad-1 asense: cgacaaatctgtaaacataATTAacaTTATGATatcgtttaatggcggac		
Mad-2 sense: ccggtttattcctaccgaatTTATAAATTTtcgattttattaccttc		
Mad-2 asense: gaaggtaataaaatcgaAAATTTATAAattcggtaggaataaaccgg		
Mad-3 sense: ccttatctatcggaccggtctTAAGTAAATAAtgtctgtctgtccccatatctttcagg		
Mad-3 asense: cctgaaagatatggggacagacagacaTTATTTACTTAagaccggtccgatagataagg		
Hox-1 Δ2 sense: agatttacgacagcatttcaCCCCttatgtcacattctaggg		
Hox-1 Δ2 asense: ccctagaatgtgacataaGGGGtgaaatgctgtcgtaaatct		
Hox-2 sense: gcgcatctccgccgtaaaccGTCGTCACGttttatgttaatgcaac		
Hox-2 asense: gttgcattaacataaaaCGTGACGACggtttacggcggagatgcgc		
Hox-3 sense: tgatctgcgatcgacccaagCGGGCATCAagcatttcataatttatgtc		
Hox-3 asense: gacataaattatgaaatgctTGATGCCCGcttgggtcgatcgcagatca		
Hox-4 sense: ggctaagcgcatctccTACTGCCCAAGGatgacatttttatgttaatgc		
Hox-4 asense: gcattaacataaaaatgtcatCCTTGGGCAGTAggagatgcgcttagcc		
Hox-5 sense: gggccatttaattgtctcgaCGTCCGGTAGTAcgctgctgagctttg		
Hox-5 asense: caaagctcagcagcgTACTACCGGACGtcgagacaattaaatggccc		
Hox-6 sense: cgaaccatttgaaaataccccgccCGCCGGCGTTCgccccgctcctattcagttgcaaa		
Hox-6 asense: tttgcaactgaataggagcggggcGAACGCCGGCGggcgggggtattttcaaatggttcg		
Recombinant DNA		
attB-hs43-nuc-lacZ	[19]	
pBPGUw (Gal4)	[47]	
Software and Algorithms		
Image J	https://imagej.nih.gov/ij/	
JASPAR	http://jaspar.genereg.net/)	
Target Explorer	http://te.cryst.bbk.ac.uk/ [48]	
Vienna *Drosophila* Resource Center	http://enhancers.starklab.org/	
Other		